PHYSICAL REVIEW D **94,** 124028 (2016)

Scalar field self-force effects on a particle orbiting a Reissner-Nordström black hole

Donato Bini*

Istituto per le Applicazioni del Calcolo "M. Picone," CNR, I-00185 Rome, Italy

Gabriel G. Carvalho†

CAPES Foundation, Ministry of Education of Brazil, Brasília, Brazil and Sapienza Università di Roma - Dipartimento di Fisica, P.le Aldo Moro 5, 00185 Rome, Italy

Andrea Geralico‡

Astrophysical Observatory of Torino, INAF, I-10025 Pino Torinese (TO), Italy

(Received 7 October 2016; published 20 December 2016)

Scalar field self-force effects on a scalar charge orbiting a Reissner-Nordström black hole are investigated. The scalar wave equation is solved analytically in a post-Newtonian framework, and the solution is used to compute the self-field (up to 7.5 post-Newtonian order) as well as the components of the self-force at the particle's location. The energy fluxes radiated to infinity and down the hole are also evaluated. Comparison with previous numerical results in the Schwarzschild case shows a reasonable agreement in both strong field and weak field regimes.

DOI: 10.1103/PhysRevD.94.124028

I. INTRODUCTION

Scalar self-force (SSF) effects arise when a scalar charge, moving along a given orbit in a curved spacetime, interacts with its own gravitational field, i.e., its self-field. The associated scalar field satisfies a d'Alembert-like equation with source term singular at the particle's position, mimicking the more interesting situation of gravitational perturbations induced by a small mass moving in a gravitational background modified by its own presence. The interaction of the particle with its own gravitational field in this case gives rise to a gravitational self-force (GSF) (see, e.g., Ref. [1] and references therein). It is a matter of fact that the latter problem is physically more interesting than the first one. However, the study of the first problem is easier than the second, even if the approaches as well as the computational techniques used in both cases are similar. This explains why in the literature the SSF problem has been considered as a preliminary study to the GSF one, scouting/solving all technical difficulties also affecting the more general gravitational perturbation problem. The existing literature on this topic is very rich. Indeed, besides the various pioneering works developing the fundamental formalism for self-force calculations in a curved spacetime [2–9], a number of interesting papers has been produced over the years, aiming at understanding self-force effects in black hole spacetimes, mostly Schwarzschild and Kerr [10–33].

The present paper concerns scalar field self-force effects on a scalar charge moving along a spatially circular equatorial orbit around a Reissner-Nordström (RN) black hole. The interaction between the particle and the background field is thus of the gravitational type only, the particle carrying no electromagnetic charge. We are interested in studying the coupling between the scalar charge of the associated field with the mass and the electromagnetic charge of the nonvacuum background, which was never explored before. This coupling can be seen as a gravitationally induced scalar interaction, which is complementary to existing studies on gravitationally induced electromagnetic radiation as well as electromagnetically induced gravitational radiation processes, initiated long ago by Zerilli and coworkers [34–36]. The only available analytical study of such a kind of perturbation problem in a RN spacetime involves an electromagnetic charge at rest in a perturbed RN spacetime [37–39], where the effect of charge induction on the horizon is investigated, too. Allowing the electromagnetic charge to move around the hole complicates matters considerably. On the other hand, having a scalar charge in circular motion is an intermediate step toward such a more general situation, the advantage of which is the possibility to perform the computations fully analytically. Switching off the black hole charge, one ends up with the corresponding SSF problem in the vacuum Schwarzschild spacetime, which has been already addressed in the literature from both analytical and numerical perspectives [14,17,20,21].

The main technical difficulties associated with self-force calculations are related to the regularization procedure of the scalar field and its derivatives, allowing one to extract

*donato.bini@gmail.com
†gabriel.carvalho@icranet.org
‡andrea.geralico@gmail.com

the correct, physically meaningful self-force components. We use the standard techniques reviewed, e.g., in Ref. [1], to compute the self-field decomposed into spherical harmonics and frequency modes and regularize it at the particle's position mode by mode by subtracting the diverging large-l limit. We analytically compute the regularized self-field [up to 7.5 post-Newtonian (PN) order] as well as the components of the self-force and compare our results with previous numerical studies in the Schwarzschild case [20,26], obtaining a good agreement. Finally, we complete our analysis by providing explicit expressions for the scalar radiation both at infinity and on the outer horizon.

II. SCALAR CHARGE IN A REISSNER-NORDSTRÖM BACKGROUND

Let us consider a Reissner-Nordström spacetime with line element written in standard Schwarzschild-like coordinates (t, r, θ, ϕ) as

$$ds^2 = -\frac{\Delta}{r^2}dt^2 + \frac{r^2}{\Delta}dr^2 + r^2(d\theta^2 + \sin^2\theta d\phi^2), \quad (2.1)$$

where $\Delta = r^2 - 2Mr + Q^2$. The condition $\Delta = 0$ defines the two horizons at radii $r_\pm = M \pm \sqrt{M^2 - Q^2} \equiv M(1 \pm \kappa)$, with $\kappa = \sqrt{1 - Q^2/M^2}$. The "extreme" case corresponds to $|Q| = M$ (or $\kappa = 0$), the two horizons coalescing into one. We find it convenient to introduce also the notation $w = 1 - \kappa^2 = (Q/M)^2$, such that $w = 0$ corresponds to the Schwarzschild limit, while $w = 1$ corresponds to the extreme RN case.

Let ψ be a (real, minimally coupled) scalar field associated with a scalar charge q moving along a circular equatorial timelike geodesic with 4-velocity $U = \Gamma(\partial_t + \Omega\partial_\phi)$ and parametric equations $x^\mu = z^\mu(\tau)$,

$$t = \Gamma\tau, \quad r = r_0, \quad \theta = \frac{\pi}{2}, \quad \phi = \Gamma\Omega\tau = \Omega t, \quad (2.2)$$

where τ denotes the proper time and the normalization factor Γ and the angular velocity Ω are conveniently written in terms of the inverse dimensionless radial distance $u = M/r$ as

$$\Gamma = \frac{1}{\sqrt{1 - 3u + 2(1 - \kappa^2)u^2}},$$
$$M\Omega = u^{3/2}\sqrt{1 - (1 - \kappa^2)u}, \quad (2.3)$$

respectively.

Assuming that the particle's field can be treated as a small perturbation on the fixed RN background implies that it obeys the massless Klein-Gordon equation

$$\Box\psi = -4\pi\varrho, \quad (2.4)$$

where

$$\Box\psi = \frac{1}{\sqrt{-g}}\partial_\mu(\sqrt{-g}g^{\mu\nu}\partial_\nu\psi) \quad (2.5)$$

is the D'Alembertian (with g denoting the determinant of the metric) and

$$\varrho(x^\mu) = q\int (-g)^{-1/2}\delta^4(x^\mu - z^\mu(\tau))d\tau$$
$$= \frac{q}{r_0^2\Gamma}\delta(r - r_0)\delta\left(\theta - \frac{\pi}{2}\right)\delta(\phi - \Omega t), \quad (2.6)$$

the charge density of the scalar particle with support only along the particle's world line (2.2). Decomposing into spherical harmonics then gives

$$\varrho = \frac{1}{4\pi r_0}\delta(r - r_0)\sum_{lm} q_{lm}e^{-im\Omega t}Y_{lm}(\theta, \phi), \quad (2.7)$$

where

$$q_{lm} = \frac{4\pi q}{r_0\Gamma}Y^*_{lm}(\pi/2, 0), \quad (2.8)$$

and similarly for the scalar field ψ, the dependence on temporal, radial, and angular variables of which can be separated as

$$\psi(t, r, \theta, \phi) = \frac{1}{2\pi}\int \sum_{lm}\psi_{lm\omega}(r)e^{-i\omega t}Y_{lm}(\theta, \phi)d\omega. \quad (2.9)$$

The wave equation (2.4) thus reduces to the following equation for the radial part,

$$\mathcal{L}_{(r)}(\psi_{lm\omega}(r)) = S_{lm\omega}\delta(r - r_0), \quad (2.10)$$

with

$$\mathcal{L}_{(r)}(\psi_{lm\omega}(r)) \equiv \frac{d^2}{dr^2}\psi_{lm\omega}(r) + \frac{2(r - M)}{\Delta}\frac{d}{dr}\psi_{lm\omega}(r)$$
$$+ \left[\frac{\omega^2 r^4}{\Delta^2} - \frac{l(l+1)}{\Delta}\right]\psi_{lm\omega}(r), \quad (2.11)$$

whereas

$$S_{lm\omega} = -2\pi\frac{r_0}{\Delta_0}q_{lm}\delta(\omega - m\Omega), \quad (2.12)$$

with $\Delta_0 = \Delta(r_0)$, comes from taking the Fourier transform of the charge density (2.7).

III. COMPUTATION OF THE SCALAR FIELD ALONG THE WORLD LINE

The radial part of the scalar field is computed by using the Green function method as

$$\psi_{lm\omega}(r) = \int G_{lm\omega}(r,r')\Delta(r')S_{lm\omega}\delta(r'-r_0)dr' \\ = G_{lm\omega}(r,r_0)\Delta_0 S_{lm\omega}, \tag{3.1}$$

where the Green function $G_{lm\omega}(r,r')$ satisfies the equation $\mathcal{L}_{(r)}(G_{lm\omega}(r,r')) = \Delta^{-1}(r')\delta(r-r')$. It reads as

$$G_{lm\omega}(r,r') = \frac{1}{W_{lm\omega}}[R_{\rm in}^{lm\omega}(r)R_{\rm up}^{lm\omega}(r')H(r'-r) \\ + R_{\rm in}^{lm\omega}(r')R_{\rm up}^{lm\omega}(r)H(r-r')], \tag{3.2}$$

where $H(x)$ denotes the Heaviside step function; $R_{\rm in}^{lm\omega}(r)$ and $R_{\rm up}^{lm\omega}(r)$ are two independent homogeneous solutions of the radial wave equation having the correct behavior at the outer horizon and at infinity, respectively; and

$$W_{lm\omega} = \Delta(r)[R_{\rm in}^{lm\omega}(r)R_{\rm up}^{\prime lm\omega}(r) - R_{\rm in}^{\prime lm\omega}(r)R_{\rm up}^{lm\omega}(r)] \tag{3.3}$$

is the associated (constant) Wronskian. Substituting then into Eq. (2.9) gives

$$\psi(x^\mu) = -\sum_{lm} G_{lm\omega}(r,r_0)|_{\omega=m\Omega} r_0 q_{lm} e^{-im\Omega t} Y_{lm}(\theta,\phi), \tag{3.4}$$

which, once evaluated along the particle world line (2.2), becomes

$$\psi_0 = -\frac{4\pi q}{\Gamma}\sum_{lm} G_{lm\omega}(r_0,r_0)|_{\omega=m\Omega}|Y_{lm}(\pi/2,0)|^2, \tag{3.5}$$

only depending on r_0. The above expression for ψ_0 actually requires taking the limit $r\to r_0^\pm$ properly, and must be suitably regularized in order to remove its singular part, because the field has a divergent behavior there.

In order to compute the Green function, we have first to solve the homogeneous radial wave equation (2.10) up to a certain PN order to obtain the in and up solutions, which are of the form

$$R_{\rm in(PN)}^{lm\omega}(r) = r^l[1 + A_2^{lm\omega}(r)\eta^2 + A_4^{lm\omega}(r)\eta^4 \\ + A_6^{lm\omega}(r)\eta^6 + A_8^{lm\omega}(r)\eta^8 + \cdots], \\ R_{\rm up(PN)}^{lm\omega}(r) = R_{\rm in(PN)}^{-l-1m\omega}(r). \tag{3.6}$$

However, these solutions do not automatically fulfill the correct boundary conditions. A consequence of this fact is the presence of diverging terms in the coefficients A_i for certain values of l. Therefore, high-order PN solutions usually require using a technique first introduced by Mano, Suzuki, and Takasugi (MST) [40,41]. We will give some detail in Appendix A.

Turning then to Eq. (3.5), the sum over m is straightforwardly computed by using standard formulas. Before summing over l, instead, one has only to remove the divergent term for large l, i.e.,

$$\psi_0^{\rm reg} = \sum_{l=0}^{\infty}(\psi_0^l - B), \tag{3.7}$$

with ψ_0 being continuous across the location of the scalar charge (see also Appendix B of Ref. [20]). The subtraction term turns out to be (in units of q)

$$B = u - \frac{1}{4}u^2 + \left(\frac{9}{64} - \frac{3}{4}\kappa^2\right)u^3 \\ + \left(-\frac{73}{32}\kappa^2 + \frac{199}{256}\right)u^4 \\ + \left(\frac{39625}{16384} - \frac{39}{64}\kappa^4 - \frac{1425}{256}\kappa^2\right)u^5 \\ + \left(-\frac{907}{256}\kappa^4 - \frac{52585}{4096}\kappa^2 + \frac{451007}{65536}\right)u^6 \\ + \left(-\frac{1926415}{65536}\kappa^2 - \frac{109317}{8192}\kappa^4 \\ + \frac{20043121}{1048576} - \frac{171}{256}\kappa^6\right)u^7 + O(u^8). \tag{3.8}$$

This can be shown to be the Taylor expansion of

$$B_{\rm analytic} = \frac{u}{\sqrt{1-3u}}\frac{\sqrt{1-\sigma}}{\Gamma}\frac{2}{\pi}{\rm EllipticK}(\sigma), \tag{3.9}$$

where

$$\sigma = \frac{u[1+u(1-\kappa^2)]}{1-2u+u^2(1-\kappa^2)}. \tag{3.10}$$

It is useful to introduce the dimensionless angular velocity variable

$$y = (M\Omega)^{2/3} = u(1+wu)^{1/3}, \tag{3.11}$$

as from Eq. (2.3), with inverse relation

$$u = y - \frac{1}{3}wy^2 + \frac{1}{3}w^2y^3 - \frac{35}{81}w^3y^4 + \frac{154}{243}w^4y^5 \\ - w^5y^6 + \frac{10868}{6561}w^6y^7 + O(y^8), \tag{3.12}$$

where we recall $w = 1-\kappa^2$.

By applying the MST technique [40,41] to the multipoles up to $l = 4$ (included), we get the following final result for the regularized field valid up to the 7.5 PN order:

$$
\begin{aligned}
\psi_0^{\rm reg} = & -y^3 + \left[\frac{35}{18} + \left(-\frac{7}{32} + \frac{w}{32}\right)\pi^2 - \frac{4}{3}\gamma - \frac{4}{3}\ln(2) - \frac{2}{3}\ln(y)\right] y^4 \\
& + \left[\frac{1141}{360} - \frac{35}{54}w + \left(\frac{29}{512} + \frac{97}{1536}w - \frac{w^2}{96}\right)\pi^2 + \left(\frac{2}{3} - \frac{8}{9}w\right)\gamma + \left(-\frac{18}{5} - \frac{8}{9}w\right)\ln(2) + \left(\frac{1}{3} - \frac{4}{9}w\right)\ln(y)\right] y^5 \\
& + \left(-\frac{38}{45} + \frac{8}{45}w\right)\pi y^{11/2} \\
& + \left[-\frac{23741}{1680} + \frac{4607}{540}w + \frac{23}{54}w^2 + \left(-\frac{279}{1024} - \frac{397}{1536}w - \frac{11}{512}w^2 + \frac{1}{96}w^3\right)\pi^2 + \left(\frac{77}{6} - \frac{46}{9}w + \frac{4}{9}w^2\right)\gamma \right. \\
& \left. + \left(\frac{1627}{42} - \frac{54}{5}w + \frac{4}{9}w^2\right)\ln(2) - \frac{729}{70}\ln(3) + \left(\frac{77}{12} - \frac{23}{9}w + \frac{2}{9}w^2\right)\ln(y)\right] y^6 \\
& + \left(-\frac{3}{35} - \frac{2696}{4725}w + \frac{16}{135}w^2\right)\pi y^{13/2} \\
& + \left\{-\frac{1515589307}{27216000} + \frac{3098381}{378000}w - \frac{3497}{3240}w^2 - \frac{793}{1458}w^3 \right. \\
& + \left(-\frac{58}{45} + \frac{8}{45}w\right)(1-w)^{3/2} - \frac{2}{3}(2-w)(1-w)\ln(1-w) \\
& + \left(-\frac{6059603}{983040} + \frac{1892003}{983040}w + \frac{2287}{9216}w^2 + \frac{871}{20736}w^3 - \frac{35}{2592}w^4\right)\pi^2 + \left(\frac{76585}{262144} - \frac{14281}{131072}w + \frac{2665}{262144}w^2\right)\pi^4 \\
& + \left[-\frac{5321}{900} + \frac{4312}{675}w - \frac{4}{27}w^2 - \frac{112}{243}w^3 + \left(\frac{152}{45} - \frac{32}{45}w\right)\gamma + \left(\frac{304}{45} - \frac{64}{45}w\right)\ln(2) + \left(\frac{152}{45} - \frac{32}{45}w\right)\ln(y)\right]\gamma \\
& + \left[-\frac{1786621}{18900} + \frac{149404}{4725}w - \frac{8}{15}w^2 - \frac{112}{243}w^3 + \left(\frac{152}{45} - \frac{32}{45}w\right)\ln(2) + \left(\frac{152}{45} - \frac{32}{45}w\right)\ln(y)\right]\ln(2) \\
& \left. + \left(\frac{12393}{140} - \frac{729}{35}w\right)\ln(3) - \frac{16}{3}\zeta(3) + \left[-\frac{10121}{1800} + \frac{4856}{675}w - \frac{38}{27}w^2 - \frac{56}{243}w^3 + \left(\frac{38}{45} - \frac{8}{45}w\right)\ln(y)\right]\ln(y)\right\} y^7 \\
& + \left(\frac{35633}{3780} - \frac{192541}{33075}w + \frac{5062}{4725}w^2 - \frac{8}{135}w^3\right)\pi y^{15/2} + O(y^8). \qquad (3.13)
\end{aligned}
$$

In the Schwarzschild case (i.e., in the limit $w \to 0$), it reduces to

$$
\begin{aligned}
\psi_0^{\rm reg,schw} = & -y^3 + \left(\frac{35}{18} - \frac{7}{32}\pi^2 - \frac{4}{3}\gamma - \frac{4}{3}\ln(2) - \frac{2}{3}\ln(y)\right) y^4 + \left(\frac{1141}{360} + \frac{29}{512}\pi^2 + \frac{2}{3}\gamma - \frac{18}{5}\ln(2) + \frac{1}{3}\ln(y)\right) y^5 - \frac{38}{45}\pi y^{11/2} \\
& + \left(-\frac{23741}{1680} - \frac{279}{1024}\pi^2 + \frac{77}{6}\gamma + \frac{1627}{42}\ln(2) - \frac{729}{70}\ln(3) + \frac{77}{12}\ln(y)\right) y^6 - \frac{3}{35}\pi y^{13/2} \\
& + \left[-\frac{1515589307}{27216000} - \frac{6059603}{983040}\pi^2 + \frac{76585}{262144}\pi^4 + \left(-\frac{5321}{900} + \frac{152}{45}\gamma + \frac{304}{45}\ln(2) + \frac{152}{45}\ln(y)\right)\gamma \right. \\
& \left. + \left(-\frac{1786621}{18900} + \frac{152}{45}\ln(2) + \frac{152}{45}\ln(y)\right)\ln(2) + \frac{12393}{140}\ln(3) - \frac{16}{3}\zeta(3) + \left(-\frac{10121}{1800} + \frac{38}{45}\ln(y)\right)\ln(y)\right] y^7 \\
& + \frac{35633}{3780}\pi y^{15/2} + O(y^8), \qquad (3.14)
\end{aligned}
$$

which was never shown before in the literature.[1] The transcendental structure of the various PN orders is highlighted by replacing ordinary logarithms by "eulerlogs," i.e.,

$$
\begin{aligned}
{\rm eulerlog}_m(x) &= \gamma + \ln(2) + \frac{1}{2}\ln(y) + \ln(m), \\
m &= 1, 2, 3, \ldots, \qquad (3.15)
\end{aligned}
$$

[1]The first terms of this expansion [up to $O(y^5)$ included] agree with unpublished results by Bini and Damour [42].

TABLE I. Comparison between the analytical prediction (3.14) for the regularized scalar field in the Schwarzschild case ($w = 0$) and the numerical values taken from Table I of Ref. [20]. The difference $\Delta\psi_0^{\rm schw} = \psi_0^{\rm schw,\,num} - \psi_0^{\rm schw}$ and the relative error $\Delta\psi_0^{\rm schw}/\psi_0^{\rm schw}$ are shown in the third and fourth columns, respectively. The superscript "reg" has been suppressed for simplicity.

y	$\psi_0^{\rm schw}$	$\Delta\psi_0^{\rm schw}$	$\Delta\psi_0^{\rm schw}/\psi_0^{\rm schw}$
1/4	−0.02304519610	-9.43×10^{-4}	0.0409
1/5	−0.01022371010	-1.05×10^{-5}	0.00102
1/6	−0.005468782560	1.40×10^{-5}	−0.00255
1/7	−0.003282635718	7.29×10^{-6}	−0.00222
1/8	−0.002130877461	3.37×10^{-6}	−0.00158
1/10	−0.001050586634	7.94×10^{-7}	-7.55×10^{-4}
1/14	$-3.701411742\times10^{-4}$	7.66×10^{-8}	-2.07×10^{-4}
1/20	$-1.246786056\times10^{-4}$	5.81×10^{-9}	-4.66×10^{-5}
1/30	$-3.661740186\times10^{-5}$	3.02×10^{-10}	-8.24×10^{-6}
1/50	$-7.889525256\times10^{-6}$	7.26×10^{-12}	-9.20×10^{-7}
1/70	$-2.877222881\times10^{-6}$	8.81×10^{-13}	-3.06×10^{-7}
1/100	$-9.884245218\times10^{-7}$	2.18×10^{-14}	-2.21×10^{-8}
1/200	$-1.239865750\times10^{-7}$	-2.50×10^{-14}	2.02×10^{-7}

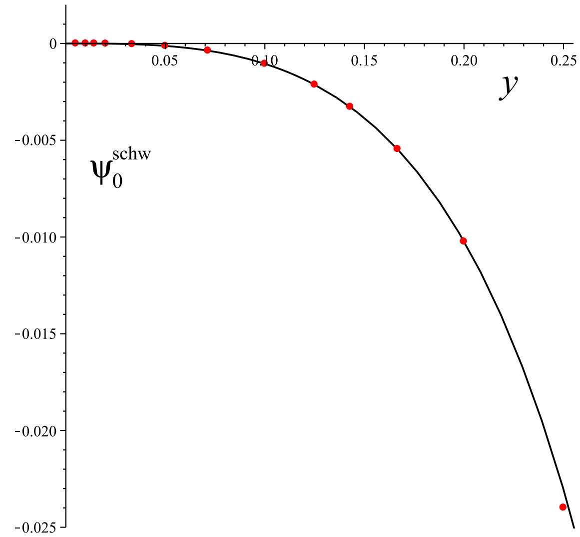

FIG. 1. The behavior of the regularized scalar field (3.14) in the Schwarzschild case ($w = 0$) as a function of y is shown in comparison with existing numerical values. The data points are taken from Table I of Ref. [20]. The superscript "reg" has been suppressed for simplicity.

first introduced in Ref. [43] in order to absorb also the Euler γ constant. For example, the lowest order $[O(y^4)]$ contains only eulerlog_1, at $O(y^5)$ a combination of eulerlog_1 and eulerlog_2 appears, etc. However, starting from $O(y^7)$, this replacement is not enough to completely remove the Euler γ terms, meaning that the transcendental structure is more involved.

Scalar self-force effects on a Schwarzschild background were numerically studied in Ref. [20]. The comparison between our analytical results and these numerical values shows a reasonable agreement (see Table I and Fig. 1). It is also interesting to study the behavior of this scalar field at the light ring $y = 1/3$ (see Ref. [44] for the case of a massive particle orbiting a Schwarzschild black hole). We provide below a simple numerical fit of the data of Table I,

$$\psi_0^{\rm reg,\,schw\ fit} = -\frac{y^3}{(1-3y)^2}(1 - 7.84y + 47.36y^2 - 8.65y^3 + 81.77y^3\ln(y)) \tag{3.16}$$

(with a maximal residual of about 2.4×10^{-4}), suggesting a blowup of the form $(1-3y)^{-2}$. However, this is an indication only, and a more conclusive statement requires strong field numerical data still currently unavailable.

Finally, in the extreme RN case (i.e., in the limit $w\to1$), we have

$$\begin{aligned}\psi_0^{\rm reg,\,extr} &= -y^3 + \left(\frac{35}{18} - \frac{3}{16}\pi^2 - \frac{4}{3}\gamma - \frac{4}{3}\ln(2) - \frac{2}{3}\ln(y)\right)y^4 + \left(\frac{2723}{1080} + \frac{7}{64}\pi^2 - \frac{2}{9}\gamma - \frac{202}{45}\ln(2) - \frac{1}{9}\ln(y)\right)y^5 \\ &\quad - \frac{2}{3}\pi y^{11/2} + \left(-\frac{78233}{15120} - \frac{555}{1024}\pi^2 + \frac{49}{6}\gamma + \frac{17881}{630}\ln(2) - \frac{729}{70}\ln(3) + \frac{49}{12}\ln(y)\right)y^6 - \frac{121}{225}\pi y^{13/2} \\ &\quad + \left[-\frac{160402001}{3265920} - \frac{438259}{110592}\pi^2 + \frac{99}{512}\pi^4 + \left(-\frac{647}{4860} + \frac{8}{3}\gamma + \frac{16}{3}\ln(2) + \frac{8}{3}\ln(y)\right)\gamma \right. \\ &\quad \left. + \left(-\frac{2174033}{34020} + \frac{8}{3}\ln(2) + \frac{8}{3}\ln(y)\right)\ln(2) + \frac{9477}{140}\ln(3) - \frac{16}{3}\zeta(3) + \left(-\frac{647}{9720} + \frac{2}{3}\ln(y)\right)\ln(y)\right]y^7 \\ &\quad + \frac{203629}{44100}\pi y^{15/2} + O(y^8).\end{aligned} \tag{3.17}$$

[Note that the term with $\ln(1-w)$ in Eq. (3.13) is proportional to $(1-w)\ln(1-w)$, which vanishes in the limit $w\to1$, so that the final expression is finite.]

IV. SCALAR SELF-FORCE

The scalar self-force is given by (see, e.g., Ref. [21])

$$F_\alpha(x^\mu) = q\nabla_\alpha\psi(x^\mu) = -q\nabla_\alpha\sum_{lm}G_{lm\omega}(r,r_0)|_{\omega=m\Omega}r_0 q_{lm}e^{-im\Omega t}Y_{lm}(\theta,\phi), \tag{4.1}$$

with nonvanishing components

$$F^0_{t(\pm)} = -\Omega F^0_{\phi(\pm)} = i\Omega\frac{4\pi q^2}{\Gamma}\sum_{lm}mG_{lm\omega}(r,r_0)|_{r=r_0^\pm,\omega=m\Omega}\times|Y_{lm}(\pi/2,0)|^2,$$
$$F^0_{r(\pm)} = -\frac{4\pi q^2}{\Gamma}\sum_{lm}\partial_r G_{lm\omega}(r,r_0)|_{r=r_0^\pm,\omega=m\Omega}|Y_{lm}(\pi/2,0)|^2, \tag{4.2}$$

once evaluated at the position of the scalar charge, i.e., in the limit $r\to r_0^\pm$. After summing over m, the divergent behavior for large l is removed by

$$F_\alpha^{0\,\mathrm{reg}} = \sum_{l=0}^\infty\left[\frac{1}{2}(F^{0l}_{\alpha(+)}+F^{0l}_{\alpha(-)})-B_\alpha\right], \tag{4.3}$$

where $F^{0l}_{\alpha(\pm)}$ denote the limits $r\to r_0^\pm$ of each mode and the l-independent quantities B_α are suitable regularization parameters, in agreement with Eq. (94) of Ref. [1], the term linear in $L=l+\frac{1}{2}$ there being removed by taking the average between the left and right limits at the particle position. The subtraction term for the radial component is given by (in units of q)

$$\begin{aligned}B_r = &-\frac{1}{2}y^2+\left(-\frac{1}{8}+\frac{1}{3}w\right)y^3+\left(-\frac{21}{128}+\frac{1}{2}w-\frac{7}{18}w^2\right)y^4+\left(-\frac{53}{512}+\frac{57}{64}w-\frac{2}{3}w^2+\frac{44}{81}w^3\right)y^5\\ &+\left(\frac{12607}{32768}+\frac{97}{96}w-\frac{331}{384}w^2+w^3-\frac{5}{6}w^4\right)y^6\\ &+\left(\frac{306759}{131072}-\frac{18433}{16384}w+\frac{4517}{2304}w^2+\frac{1055}{864}w^3-\frac{130}{81}w^4+\frac{988}{729}w^5\right)y^7+O(y^8),\end{aligned} \tag{4.4}$$

whereas $B_t=0$.

The final result for the regularized temporal and radial components of the self-force valid through the order $O(y^{15/2})$ is (in units of q)

$$\begin{aligned}F_t^{0\,\mathrm{reg}} = &\frac{1}{3}y^4+\left(-\frac{1}{6}+\frac{2}{9}w\right)y^5+\frac{2}{3}\pi y^{11/2}+\left(-\frac{77}{24}+\frac{23}{18}w-\frac{1}{9}w^2\right)y^6+\left(\frac{9}{5}+\frac{4}{9}w\right)\pi y^{13/2}\\ &+\left[\frac{7721}{3600}-\frac{1753}{675}w+\frac{10}{27}w^2+\frac{28}{243}w^3+\frac{2}{3}(1-w)^{3/2}+\frac{4}{9}\pi^2+\left(-\frac{76}{45}+\frac{16}{45}w\right)\gamma+\left(-\frac{76}{45}+\frac{16}{45}w\right)\ln(2)\right.\\ &\left.+\left(-\frac{38}{45}+\frac{8}{45}w\right)\ln(y)\right]y^7+\left(-\frac{3761}{420}+\frac{27}{5}w-\frac{2}{9}w^2\right)\pi y^{15/2}+O(y^8),\\ F_r^{0\,\mathrm{reg}} = &\left[-\frac{2}{9}+\left(\frac{7}{64}-\frac{1}{64}w\right)\pi^2-\frac{4}{3}\gamma-\frac{4}{3}\ln(2)-\frac{2}{3}\ln(y)\right]y^5\\ &+\left[\frac{604}{45}-\frac{41}{27}w+\left(\frac{29}{1024}-\frac{239}{3072}w+\frac{1}{96}w^2\right)\pi^2-\left(\frac{14}{3}+\frac{4}{9}w\right)\gamma-\left(\frac{66}{5}+\frac{4}{9}w\right)\ln(2)-\left(\frac{7}{3}+\frac{2}{9}w\right)\ln(y)\right]y^6\\ &+\left(-\frac{38}{45}+\frac{8}{45}w\right)\pi y^{13/2}\\ &+\left[\frac{1511}{140}+\frac{473}{90}w+\frac{103}{81}w^2+\left(\frac{1335}{2048}-\frac{1}{16}w+\frac{151}{2304}w^2-\frac{7}{576}w^3\right)\pi^2+\left(\frac{31}{2}-\frac{28}{3}w+\frac{8}{27}w^2\right)\gamma\right.\\ &\left.+\left(\frac{857}{14}-\frac{268}{15}w+\frac{8}{27}w^2\right)\ln(2)-\frac{2187}{70}\ln(3)+\left(\frac{31}{4}-\frac{14}{3}w+\frac{4}{27}w^2\right)\ln(y)\right]y^7\\ &+\left(-\frac{139}{35}+\frac{2378}{4725}w+\frac{8}{135}w^2\right)\pi y^{15/2}+O(y^8),\end{aligned} \tag{4.5}$$

respectively.

TABLE II. Comparison between the analytical expressions (4.6) for the regularized temporal and radial components of the self-force (in units of q, the superscript reg being suppressed for simplicity) in the Schwarzschild case ($w = 0$) and the numerical values taken from Tables II and III of Ref. [26]. The second and third columns display the values obtained by our analytical expressions, whereas the fourth and fifth columns display the difference with the corresponding numerical values (i.e., $\Delta F_t^{0\,\mathrm{schw}} = F_t^{0\,\mathrm{schw,num}} - F_t^{0\,\mathrm{schw}}$ and $\Delta F_r^{0\,\mathrm{schw}} = F_r^{0\,\mathrm{schw,num}} - F_t^{0\,\mathrm{schw}}$). Finally, the last two columns show the associated relative errors $\Delta F_t^{0\,\mathrm{schw}}/F_t^{0\,\mathrm{schw}}$ and $\Delta F_r^{0\,\mathrm{schw}}/F_r^{0\,\mathrm{schw}}$, respectively.

y	$F_t^{0\,\mathrm{schw}}$	$F_r^{0\,\mathrm{schw}}$	$\Delta F_t^{0\,\mathrm{schw}}$	$\Delta F_r^{0\,\mathrm{schw}}$	$\Delta F_t^{0\,\mathrm{schw}}/F_t^{0\,\mathrm{schw}}$	$\Delta F_r^{0\,\mathrm{schw}}/F_r^{0\,\mathrm{schw}}$
1/6	$3.088678309 \times 10^{-4}$	$2.069192430 \times 10^{-4}$	5.20×10^{-5}	-3.92×10^{-5}	0.168	−0.189
1/7	$1.621300383 \times 10^{-4}$	$9.086682872 \times 10^{-5}$	1.46×10^{-5}	-1.24×10^{-5}	0.0901	−0.136
1/8	$9.278324817 \times 10^{-5}$	$4.535558187 \times 10^{-5}$	4.94×10^{-6}	-4.53×10^{-6}	0.0532	−0.0999
1/10	$3.667967766 \times 10^{-5}$	$1.462629728 \times 10^{-5}$	8.23×10^{-7}	-8.42×10^{-7}	0.0224	−0.0576
1/14	$9.180183375 \times 10^{-6}$	$2.785864322 \times 10^{-6}$	5.66×10^{-8}	-6.58×10^{-8}	0.00616	−0.0236
1/20	$2.148236416 \times 10^{-6}$	$4.981418996 \times 10^{-7}$	3.36×10^{-9}	-4.35×10^{-9}	0.00156	−0.00874
1/30	$4.175425467 \times 10^{-7}$	$7.191466709 \times 10^{-8}$	1.36×10^{-10}	-1.96×10^{-10}	3.26×10^{-4}	−0.00272
1/50	$5.359926673 \times 10^{-8}$	$6.350626477 \times 10^{-9}$	2.40×10^{-12}	-3.93×10^{-12}	4.47×10^{-5}	-6.18×10^{-4}
1/70	$1.391199738 \times 10^{-8}$	$1.284814550 \times 10^{-9}$	1.67×10^{-13}	-3.15×10^{-13}	1.20×10^{-5}	-2.45×10^{-4}
1/100	$3.335029050 \times 10^{-9}$	$2.356682550 \times 10^{-10}$	9.90×10^{-15}	-6.83×10^{-14}	2.97×10^{-6}	-2.90×10^{-4}

In the Schwarzschild limit ($w \to 0$), we have

$$\begin{aligned} F_t^{0\,\mathrm{reg,schw}} &= \frac{1}{3}y^4 - \frac{1}{6}y^5 + \frac{2}{3}\pi y^{11/2} - \frac{77}{24}y^6 + \frac{9}{5}\pi y^{13/2} + \left[\frac{10121}{3600} + \frac{4}{9}\pi^2 - \frac{76}{45}\gamma - \frac{76}{45}\ln(2) - \frac{38}{45}\ln(y)\right] y^7 \\ &\quad - \frac{3761}{420}\pi y^{15/2} + O(y^8), \\ F_r^{0\,\mathrm{reg,schw}} &= \left[-\frac{2}{9} + \frac{7}{64}\pi^2 - \frac{4}{3}\gamma - \frac{4}{3}\ln(2) - \frac{2}{3}\ln(y)\right] y^5 + \left[\frac{604}{45} + \frac{29}{1024}\pi^2 - \frac{14}{3}\gamma - \frac{66}{5}\ln(2) - \frac{7}{3}\ln(y)\right] y^6 \\ &\quad - \frac{38}{45}\pi y^{13/2} + \left[\frac{1511}{140} + \frac{1335}{2048}\pi^2 + \frac{31}{2}\gamma + \frac{857}{14}\ln(2) - \frac{2187}{70}\ln(3) + \frac{31}{4}\ln(y)\right] y^7 - \frac{139}{35}\pi y^{15/2} + O(y^8). \end{aligned} \tag{4.6}$$

The leading 3PN and 4PN terms of the previous expressions agree with those of Ref. [21]. Furthermore, the comparison with available numerical results of Refs. [20,26] shows again a good agreement (see Table II and Fig. 2, where we refer to the most recent work [26]).

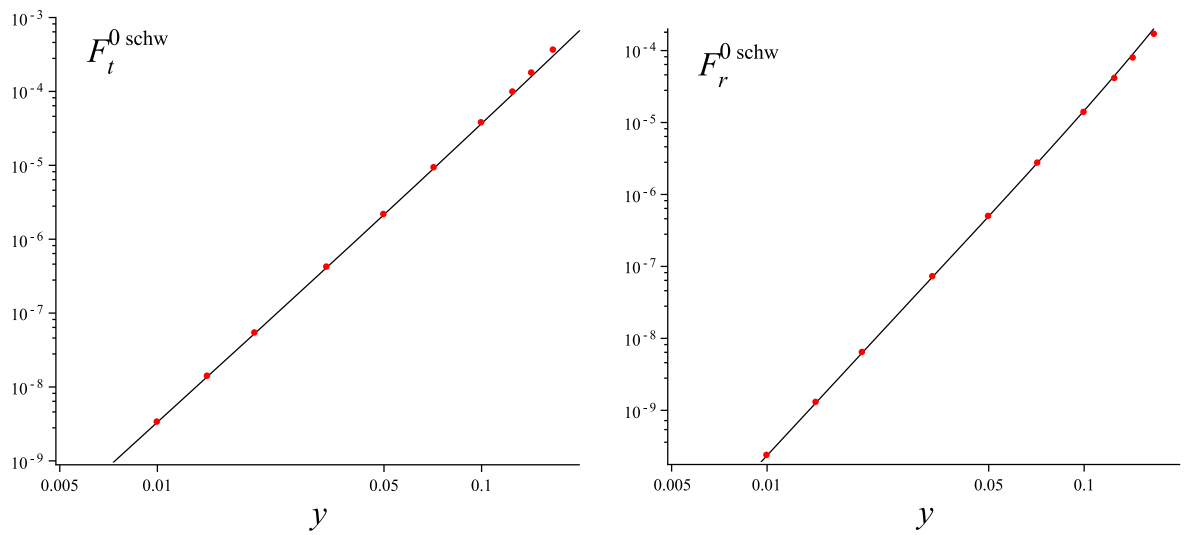

FIG. 2. Comparison of numerical data from Ref. [26] for the regularized temporal and radial components of the self-force (in units of q, the superscript reg being suppressed for simplicity) in the Schwarzschild case ($w = 0$) with the behavior of the corresponding analytical expressions (4.6).

V. SCALAR RADIATION

Let us compute the amount of scalar radiation either flowing into the hole or transmitted at spatial infinity. We need to construct the solution to the nonhomogeneous wave equation (2.10) which satisfies purely ingoing-wave boundary conditions at the black hole horizon and purely outgoing-wave boundary conditions at infinity. This is accomplished by using the two kinds of solutions $R^{H,\infty}_{lm\omega}$ to the corresponding homogeneous equation with asymptotic behavior [45–47]

$$R^H_{lm\omega} \to \begin{cases} B^{\rm trans} e^{-i\omega r_*}, & r\to r_+ \\ B^{\rm ref}\frac{e^{i\omega r_*}}{r} + B^{\rm inc}\frac{e^{-i\omega r_*}}{r}, & r\to\infty \end{cases},$$
$$R^\infty_{lm\omega} \to \begin{cases} C^{\rm up} e^{i\omega r_*} + C^{\rm ref} e^{-i\omega r_*}, & r\to r_+ \\ C^{\rm trans}\frac{e^{i\omega r_*}}{r}, & r\to\infty \end{cases}, \tag{5.1}$$

where r_* is the tortoiselike coordinate defined by $dr_*/dr = r^2/\Delta$, i.e.,

$$r_* = r + \frac{2Mr_+}{r_+ - r_-}\ln\frac{r-r_+}{2M} - \frac{2Mr_-}{r_+ - r_-}\ln\frac{r-r_-}{2M}. \tag{5.2}$$

The final solution is given by [48]

$$R_{lm\omega}(r) = Z^H_{lm\omega}(r)R^\infty_{lm\omega}(r) + Z^\infty_{lm\omega}(r)R^H_{lm\omega}(r), \tag{5.3}$$

where

$$Z^H_{lm\omega}(r) = \frac{-1}{W_{lm\omega}}\int_{r_+}^{r} R^H_{lm\omega}(r')\Delta(r')S_{lm\omega}\delta(r'-r_0)dr',$$
$$Z^\infty_{lm\omega}(r) = \frac{-1}{W_{lm\omega}}\int_{r}^{\infty} R^\infty_{lm\omega}(r')\Delta(r')S_{lm\omega}\delta(r'-r_0)dr', \tag{5.4}$$

and $W_{lm\omega} = 2i\omega C^{\rm trans}B^{\rm inc}$ is the constant Wronskian. The asymptotic behaviors of $R_{lm\omega}$ at the horizon and at infinity are then

$$R_{lm\omega}(r\to r_+) \to B^{\rm trans} Z^\infty_{lm\omega}(r_+)e^{-i\omega r_*},$$
$$R_{lm\omega}(r\to \infty) \to C^{\rm trans} Z^H_{lm\omega}(\infty)\frac{e^{i\omega r_*}}{r}, \tag{5.5}$$

respectively, so that one can define the amplitudes

$$\mathcal{Z}^H_{lm\omega} = B^{\rm trans}Z^\infty_{lm\omega}(r_+),\ \mathcal{Z}^\infty_{lm\omega} = C^{\rm trans}Z^H_{lm\omega}(\infty). \tag{5.6}$$

Explicitly, we find

$$\mathcal{Z}^H_{lm\omega} = 2\pi\frac{B^{\rm trans}}{W_{lm\omega}}r_0 q_{lm\omega}R^\infty_{lm\omega}(r_0)\delta(\omega - m\Omega) \equiv 2\pi\tilde{\mathcal{Z}}^H_{lm}\delta(\omega-m\Omega),$$
$$\mathcal{Z}^\infty_{lm\omega} = 2\pi\frac{C^{\rm trans}}{W_{lm\omega}}r_0 q_{lm\omega}R^H_{lm\omega}(r_0)\delta(\omega - m\Omega) \equiv 2\pi\tilde{\mathcal{Z}}^\infty_{lm}\delta(\omega-m\Omega). \tag{5.7}$$

The energy flux at infinity is thus given by [45–47]

$$\frac{dE^\infty}{dt} = \sum_{lm}\frac{\omega^2}{4\pi}|\tilde{\mathcal{Z}}^\infty_{lm}|^2, \tag{5.8}$$

while the energy flux at the event horizon is

$$\frac{dE^H}{dt} = \sum_{lm}\frac{M\omega^2 r_+}{2\pi}|\tilde{\mathcal{Z}}^H_{lm}|^2, \tag{5.9}$$

with $\tilde{\mathcal{Z}}^{H,\infty}_{lm}$ defined in Eq. (5.7) and $\omega = m\Omega$.

For the computation of the amplitudes and the transmission coefficients, we have used the MST ingoing and upgoing solutions, which satisfy the proper boundary conditions at the horizon and at infinity for any given value of l, i.e., $R^H_{lm\omega}(r) = R^{\rm in(MST)}_{lm\omega}(r)$ and $R^\infty_{lm\omega}(r) = R^{\rm up(MST)}_{lm\omega}(r)$. The corresponding transmission coefficients are given by [48]

$$B^{\rm trans} = e^{i\frac{\kappa}{2}(\epsilon+\tau)(1+\frac{2\ln\kappa}{1+\kappa})}\sum_{n=-\infty}^{\infty}a_n,$$
$$C^{\rm trans} = \omega^{-1}e^{i\epsilon(\ln\epsilon - \frac{1-\kappa}{2})}A^\nu_-, \tag{5.10}$$

where

$$A^\nu_- = 2^{-1+i\epsilon}e^{-\frac{\pi}{2}i(\nu+1)}e^{-\frac{\pi}{2}\epsilon}\sum_{n=-\infty}^{\infty}(-1)^n\frac{(\nu+1-i\epsilon)_n}{(\nu+1+i\epsilon)_n}a_n. \tag{5.11}$$

The definitions of the various quantities ϵ, τ, ν, a_n are given in Appendix A 2 for convenience.

We find (in units of q)

$$
\begin{aligned}
\frac{dE^\infty}{dt} &= \left(\frac{dE^\infty}{dt}\right)_N \Bigg\{1 + \left(-2+\frac{2}{3}w\right)y + 2\pi y^{3/2} + \left(-10+\frac{13}{3}w-\frac{1}{3}w^2\right)y^2 + \left(\frac{12}{5}+\frac{4}{3}w\right)\pi y^{5/2} \\
&\quad + \bigg[\frac{1331}{75}-\frac{2203}{225}w+\frac{4}{9}w^2+\frac{28}{81}w^3+\frac{4}{3}\pi^2 \\
&\quad + \left(-\frac{76}{15}+\frac{16}{15}w\right)\gamma + \left(-\frac{76}{15}+\frac{16}{15}w\right)\ln(2) + \left(-\frac{38}{15}+\frac{8}{15}w\right)\ln(y)\bigg]y^3 \\
&\quad + \left(-\frac{521}{14}+\frac{86}{5}w-\frac{2}{3}w^2\right)\pi y^{7/2} + O(y^4)\Bigg\}, \\
\frac{dE^H}{dt} &= \left(\frac{dE^\infty}{dt}\right)_N 2(1-w)(1+\sqrt{1-w})\Bigg\{y^3 + \left(2-\frac{4}{3}w\right)y^4 + \left(3-\frac{7}{3}w+2w^2\right)y^5 \\
&\quad + \bigg[\frac{1231}{75}-\frac{793}{225}w+\frac{32}{9}w^2-\frac{260}{81}w^3+\frac{1}{1-w}+\left(-\frac{38}{15}+\frac{8}{15}w\right)\ln(1-w)+\frac{1}{(1-w)^{1/2}}\left(\frac{4}{3}-\frac{2}{3}w\right)\pi^2 \\
&\quad -\frac{8}{3}\gamma + \left(-\frac{116}{15}+\frac{16}{15}w\right)\ln(2) + \left(-\frac{32}{5}+\frac{16}{15}w\right)\ln(y)\bigg]y^6 \\
&\quad + \bigg[\frac{1769}{225}-\frac{46}{15}w+\frac{907}{675}w^2-\frac{473}{81}w^3+\frac{1309}{243}w^4+\frac{1}{1-w}\left(4-\frac{10}{3}w\right)+\left(-\frac{76}{15}+\frac{40}{9}w-\frac{32}{45}w^2\right)\ln(1-w) \\
&\quad + \frac{1}{(1-w)^{1/2}}\left(\frac{8}{3}-\frac{28}{9}w+\frac{8}{9}w^2\right)\pi^2 + \left(\frac{64}{15}+\frac{8}{9}w\right)\gamma + \left(-\frac{88}{15}+\frac{88}{9}w-\frac{64}{45}w^2\right)\ln(2) \\
&\quad + \left(-8+\frac{28}{3}w-\frac{64}{45}w^2\right)\ln(y)\bigg]y^7 \\
&\quad + \left(-\frac{56}{45}+\frac{16}{45}w\right)\pi y^{15/2} \\
&\quad + \bigg[-\frac{208762}{7875}+\frac{10034656}{165375}w-\frac{4518949}{165375}w^2+\frac{1162}{675}w^3+10w^4-\frac{28}{3}w^5+\frac{1}{1-w}\left(9-\frac{44}{3}w+\frac{25}{3}w^2\right) \\
&\quad + \left(-\frac{1818}{175}+\frac{17086}{1575}w-\frac{10804}{1575}w^2+\frac{16}{15}w^3\right)\ln(1-w) + \frac{1}{(1-w)^{1/2}}\left(\frac{36}{5}-\frac{446}{45}w+\frac{262}{45}w^2-\frac{4}{3}w^3\right)\pi^2 \\
&\quad + \left(\frac{608}{105}-\frac{344}{45}w-\frac{8}{9}w^2\right)\gamma + \left(-\frac{1124}{75}+\frac{22132}{1575}w-\frac{23008}{1575}w^2+\frac{32}{15}w^3\right)\ln(2) \\
&\quad + \left(-\frac{9388}{525}+\frac{3128}{175}w-\frac{7436}{525}w^2+\frac{32}{15}w^3\right)\ln(y)\bigg]y^8 \\
&\quad + \left(\frac{88}{225}+\frac{196}{675}w-\frac{16}{135}w^2\right)\pi y^{17/2} + O(y^9)\Bigg\},
\end{aligned} \tag{5.12}
$$

where

$$\left(\frac{dE^\infty}{dt}\right)_N = \frac{1}{3}y^4, \tag{5.13}$$

in terms of the gauge-invariant variable y [see Eq. (3.12)]. Note that the flux at infinity is computed up to the 3.5PN order, i.e., at $O(y^{7/2})$ included (see Appendix B). The leading contribution to the flux on the horizon, instead, enters at 3PN order beyond the lowest order and is computed through $O(y^{17/2})$.

In the Schwarzschild case ($w \to 0$), the previous expressions reduce to

$$\frac{dE^\infty}{dt} = \left(\frac{dE^\infty}{dt}\right)_N \left[1 - 2y + 2\pi y^{3/2} - 10y^2 + \frac{12}{5}\pi y^{5/2} + \left(\frac{1331}{75} + \frac{4}{3}\pi^2 - \frac{76}{15}\gamma - \frac{76}{15}\ln(2) - \frac{38}{15}\ln(y)\right)y^3 - \frac{521}{14}\pi y^{7/2} + O(y^4)\right],$$

$$\frac{dE^H}{dt} = \left(\frac{dE^\infty}{dt}\right)_N 4y^3 \left[1 + 2y + 3y^2 + \left(\frac{1306}{75} + \frac{4}{3}\pi^2 - \frac{8}{3}\gamma - \frac{116}{15}\ln(2) - \frac{32}{5}\ln(y)\right)y^3 + \left(\frac{2669}{225} + \frac{8}{3}\pi^2 + \frac{64}{15}\gamma - \frac{88}{15}\ln(2) - 8\ln(y)\right)y^4 - \frac{56}{45}\pi y^{9/2} + \left(-\frac{137887}{7875} + \frac{36}{5}\pi^2 + \frac{608}{105}\gamma - \frac{1124}{75}\ln(2) - \frac{9388}{525}\ln(y)\right)y^5 + \frac{88}{225}\pi y^{11/2} + O(y^6)\right], \tag{5.14}$$

whereas in the extreme RN case ($w \to 1$), we have

$$\frac{dE^\infty}{dt} = \left(\frac{dE^\infty}{dt}\right)_N \left[1 - \frac{4}{3}y + 2\pi y^{3/2} - 6y^2 + \frac{56}{15}\pi y^{5/2} + \left(\frac{3542}{405} + \frac{4}{3}\pi^2 - 4\gamma - 4\ln(2) - 2\ln(y)\right)y^3 - \frac{4343}{210}\pi y^{7/2} + O(y^4)\right],$$

$$\frac{dE^H}{dt} = \left(\frac{dE^\infty}{dt}\right)_N 2y^6 \left[1 + \frac{2}{3}y + \frac{8}{3}y^2 + O(y^3)\right]. \tag{5.15}$$

Therefore, when the black hole is extremely charged, the horizon-absorbed flux starts three more PN orders beyond with respect to the nonextreme case.

We show in Table III the comparison between the total energy flux

$$\frac{dE^{\rm tot}}{dt} = \frac{dE^\infty}{dt} + \frac{dE^H}{dt} \tag{5.16}$$

computed by using Eq. (5.14) in the Schwarzschild case and the numerical values taken from Table I of Ref. [26]. We find that the agreement is reasonably good in the weak field regime, with fractional errors ranging from 10^{-1} (at $y = 1/6$) to 10^{-4} (at $y = 1/40$). Furthermore, we have checked that our analytic expression (5.16) for the total energy flux agrees with the analogous quantity obtained from the self-force energy balance relation $dE^{\rm tot}/dt = \Gamma^{-1}F_t^{0\,\rm reg}$ up to the order $O(y^8)$, which is our accuracy in the computation of the self-force components [see Eq. (4.6)].

TABLE III. Comparison between the total energy flux $\dot{E}^{\rm tot} = \dot{E}^\infty + \dot{E}^H$ (in units of q, the overdot denoting d/dt) computed by using the analytical expressions (5.14) in the Schwarzschild case ($w = 0$) and the numerical values taken from Table I of Ref. [26]. The last two columns display the difference $\Delta\dot{E}^{\rm tot} = \dot{E}^{\rm tot,num} - \dot{E}^{\rm tot}$ and the corresponding relative error $\Delta\dot{E}^{\rm tot}/\dot{E}^{\rm tot}$.

y	$\dot{E}^{\rm tot}$	$\Delta\dot{E}^{\rm tot}$	$\Delta\dot{E}^{\rm tot}/\dot{E}^{\rm tot}$
1/6	$2.174332404 \times 10^{-4}$	3.78×10^{-5}	0.174
1/8	$7.334363785 \times 10^{-5}$	3.91×10^{-6}	0.0533
1/10	$3.06988477 \times 10^{-5}$	6.78×10^{-7}	0.0221
1/20	$1.980748387 \times 10^{-6}$	2.92×10^{-9}	0.00147
1/40	$1.262548016 \times 10^{-7}$	-2.81×10^{-11}	-2.22×10^{-4}

Finally, we note that the (dimensionless) angular momentum fluxes can be easily calculated through [48]

$$\frac{dJ^{H,\infty}}{dt} = y^{-3/2}\frac{dE^{H,\infty}}{dt}. \tag{5.17}$$

VI. CONCLUDING REMARKS

We have analyzed self-force effects on a scalar charge moving along a circular orbit around a Reissner-Nordström black hole. The scalar wave equation is separated by using standard spherical harmonics (available here because of the underlying spherical symmetry of the background), and the field is decomposed into frequency modes. The associated radial equation is solved perturbatively in a PN framework by using the Green function method. The scalar field as well as the components of the self-force are then regularized at the particle's position by subtracting the divergent term mode by mode, summing then the infinite series up to a certain PN order. The MST approach has also been adopted for computing a number of radiative multipoles (up to $l = 4$), so that our final result for the field is accurate up to the 7.5PN order, i.e., up to the order $O(y^{15/2})$ included in terms of the dimensionless gauge-invariant frequency variable $y = (M\Omega)^{2/3}$. Since the scalar charge interacts only gravitationally with the background field, the coupling with the black hole electromagnetic charge is quadratic. The two limiting cases of a Schwarzschild black hole (which was missing in the literature and represents by itself an interesting byproduct of our work) and of an extreme Reissner-Nordström black hole are discussed explicitly. The comparison of the analytically computed regularized field and self-force components with existing numerical results in the Schwarzschild case [17,26] has shown a good agreement (see Tables I and II). We have also evaluated the radiation fluxes both at infinity and on the outer horizon up to $O(y^{7/2})$ and $O(y^{17/2})$ included, respectively. We have found that, when the black hole is extremely charged, the horizon-absorbed flux starts three more PN orders beyond than the nonextreme case. The problem of radiation due to an electromagnetic charge orbiting a RN black hole generalizing the present analysis will be considered in future works.

ACKNOWLEDGMENTS

B. D. thanks ICRANet for partial support. G. G. C. is grateful to the Brazilian agency CAPES for the financial support in form of a doctoral scholarship BEX-15114/13-9. All authors thank Prof. T. Damour for useful comments.

APPENDIX A: HOMOGENEOUS SOLUTIONS TO THE SCALAR WAVE EQUATION

1. PN solutions

PN solutions have the form (3.6), i.e.,

$$\begin{aligned} R^{lm\omega}_{\mathrm{in(PN)}}(r) &= r^l[1 + A_2^{lm\omega}(r)\eta^2 + A_4^{lm\omega}(r)\eta^4 + A_6^{lm\omega}(r)\eta^6 \\ &\quad + A_8^{lm\omega}(r)\eta^8 + \ldots], \\ R^{lm\omega}_{\mathrm{up(PN)}}(r) &= R^{-l-1m\omega}_{\mathrm{in(PN)}}(r). \end{aligned} \tag{A1}$$

The first coefficients are given by

$$\begin{aligned} A_2^{lm\omega}(r) &= -\frac{Ml}{r} - \frac{\omega^2 r^2}{2(2l+3)}, \\ A_4^{lm\omega}(r) &= \frac{M^2}{r^2}\frac{l(l-1)(2l-1-\kappa^2)}{2(2l-1)} + M\omega^2 r\frac{l^2-5l-10}{2(2l+3)(l+1)} + \frac{\omega^4 r^4}{8(2l+3)(2l+5)}, \\ A_6^{lm\omega}(r) &= -\frac{M^3}{r^3}\frac{l(l-1)(l-2)(2l-1-3\kappa^2)}{6(2l-1)} - 2M^2\omega^2\frac{[3(2l-1)(2l+3)+(3l^2+3l-2)\kappa^2][(2l+1)\ln(r/R)-1]}{(2l-1)(2l+3)(2l+1)^2} \\ &\quad - M\omega^4 r^3\frac{3l^3-27l^2-142l-136}{24(l+1)(l+2)(2l+3)(2l+5)} - \frac{\omega^6 r^6}{48(2l+3)(2l+5)(2l+7)}, \\ A_8^{lm\omega}(r) &= \frac{M^4}{r^4}\frac{l(l-1)(l-2)(l-3)}{24(2l-1)(2l-3)}[(2l-1)(2l-3)-3\kappa^2(4l-6-\kappa^2)] \\ &\quad + \frac{M^3\omega^2}{r}\left\{-\frac{4l^6-32l^5-99l^4-241l^3-436l^2-276l-36}{6l(2l+3)(2l+1)^2} + \frac{48l^5+348l^4+540l^3+126l^2-120l-36}{6l(2l+3)(2l-1)(2l+1)^2}\kappa^2 \right. \\ &\quad \left. + \left[\frac{6l}{2l+1} + \frac{2l(3l^2+3l-2)}{(2l+3)(2l-1)(2l+1)}\kappa^2\right]\ln(r/R)\right\} \\ &\quad + M^2\omega^2 r^2\left\{-\frac{24l^7+156l^6-1766l^5-13267l^4-29512l^3-23465l^2-2058l+2784}{48(l+1)(2l+3)^2(2l+5)(2l+1)^2(l+2)} \right. \\ &\quad + \frac{16l^6+80l^5-440l^4-2432l^3-2803l^2+11l+784}{16(2l-1)(2l+3)^3(2l+5)(2l+1)^2}\kappa^2 \\ &\quad \left. + \left[\frac{3}{(2l+3)(2l+1)} + \frac{3l^2+3l-2}{(2l-1)(2l+3)^2(2l+1)}\kappa^2\right]\ln(r/R)\right\} \\ &\quad + M\omega^6 r^5\frac{5l^4-60l^3-625l^2-1548l-1108}{240(l+3)(l+2)(2l+7)(2l+5)(2l+3)(l+1)} + \frac{\omega^8 r^8}{384(2l+9)(2l+7)(2l+5)(2l+3)}, \end{aligned} \tag{A2}$$

where R is a length scale. This solution, which we need, however, to compute the sum over all multipoles, becomes immediately inadequate, and one should use the MST technique. In fact, the coefficient A_4 of the "up" solution [obtained from $A_4^{lm\omega}(r)$ with $l \to -l-1$] diverges for $l=0$; similarly, higher order coefficients diverge for $l = 1, 2, \ldots$, etc.

2. MST solutions

The MST technique [40,41] allows one to find a homogeneous solution to the radial equation which satisfies retarded boundary conditions at the horizon $[R^{lm\omega}_{\rm in(MST)}(r)]$ and radiative boundary conditions at infinity $[R^{lm\omega}_{\rm up(MST)}(r)]$.

The ingoing solution can be formally written as a convergent (at any finite value of r) series of hypergeometric functions,

$$R^{lm\omega}_{\rm in(MST)}(x) = C_{\rm (in)}(x) \sum_{n=-\infty}^{\infty} a_n F(n+\nu+1-i\tau, -n-\nu - i\tau, 1-i\epsilon-i\tau; x), \tag{A3}$$

with

$$C_{\rm (in)}(x) = e^{i\epsilon\kappa x}(-x)^{-i(\epsilon+\tau)/2}(1-x)^{i(\epsilon-\tau)/2}, \tag{A4}$$

where the new variable $x = (r_+ - r)/2M\kappa$ has been introduced and

$$\epsilon = 2M\omega, \qquad \tau = \frac{1}{2}\frac{\epsilon(\kappa^2+1)}{\kappa}. \tag{A5}$$

The hypergeometric functions above are better evaluated by using the standard identity

$$F(a,b;c;x) = y^a \frac{\Gamma(c)\Gamma(b-a)}{\Gamma(b)\Gamma(c-a)} F(a, c-b, a-b+1; y) + y^b \frac{\Gamma(c)\Gamma(a-b)}{\Gamma(a)\Gamma(c-b)} F(b, c-a, b-a+1; y), \tag{A6}$$

involving the "small" variable $y = 1/(1-x)$. Note that the overall factor $\Gamma(c)$ does not depend on n, so that it can be factored out.

The expansion coefficients a_n satisfy the following three-term recurrence relation

$$\alpha_n^\nu a_{n+1} + \beta_n^\nu a_n + \gamma_n^\nu a_{n-1} = 0, \tag{A7}$$

where

$$\begin{aligned}
\alpha_n^\nu &= \frac{i\epsilon\kappa(n+\nu+1+i\epsilon)(n+\nu+1-i\epsilon)(n+\nu+1+i\tau)}{(n+\nu+1)(2n+2\nu+3)}, \\
\beta_n^\nu &= -l(l+1) + (n+\nu)(n+\nu+1) + \epsilon\kappa\tau + \epsilon^2 + \frac{\epsilon^3\kappa\tau}{(n+\nu)(n+\nu+1)}, \\
\gamma_n^\nu &= -\frac{i\epsilon\kappa(n+\nu+i\epsilon)(n+\nu-i\tau)(n+\nu-i\epsilon)}{(n+\nu)(2n+2\nu-1)}.
\end{aligned} \tag{A8}$$

Once the recurrence system has been solved for $n = 1 \ldots N$ and $n = -N \ldots -1$ for a given N such that $a_N = 0 = a_{-N}$, the case $n = 0$ with $a_0 = 1$ becomes a compatibility condition which yields the parameter

$$\nu = l + \sum_{k=1}^{\infty} \nu_k \epsilon^{2k}. \tag{A9}$$

The solution of the recurrence system is rather involved (even in this relatively simple case). The structure of the expansion coefficients

$$a_n = \sum_{k=i}^{j} c_{nk}\epsilon^k \tag{A10}$$

is summarized in Table IV for $l = 1$ and $N = 15$, as an example.

The upgoing solution can be formally written as a convergent (at spatial infinity) series of irregular confluent hypergeometric functions with the same series coefficients,

$$R^{lm\omega}_{\rm up(MST)}(z) = C_{\rm (up)}(z) \sum_{n=-\infty}^{\infty} a_n \frac{(\nu+1-i\epsilon)_n}{(\nu+1+i\epsilon)_n}(2iz)^n \Psi[n+\nu+1-i\epsilon, 2n+2\nu+2; -2iz], \tag{A11}$$

with

$$C_{\rm (up)}(z) = (2z)^\nu e^{-\pi\epsilon} e^{-i\pi(\nu+1)} e^{iz}\left(1 - \frac{\epsilon\kappa}{z}\right)^{-i(\epsilon+\tau)/2}, \tag{A12}$$

where the new variable $z = \omega(r - r_-) = \epsilon\kappa(1-x)$ has been introduced and $(A)_n = \Gamma(A+n)/\Gamma(A)$ is the Pochammer symbol. The irregular confluent hypergeometric functions above can be conveniently split into two pieces by using the identity

TABLE IV. The structure of the expansion coefficients (A10) of the recurrence relation is shown for $l = 1$ and $N = 15$, so that $a_{-15} = 0 = a_{15}$ and $a_0 = 1$.

n	−14	−13	−12	−11	−10	−9	−8	−7	−6	−5	−4	−3	−2	−1	0	1	2	3	4	5	6	7	8	9	10	11	12	13	14
i	13	12	11	10	9	8	7	6	5	4	3	2	3	1	···	1	2	3	4	5	6	7	8	9	10	11	12	13	14
j	14	14	14	14	14	14	14	14	14	14	14	14	14	14	···	14	14	14	14	14	14	14	14	14	14	14	14	14	14

$$\Psi(a,b;\zeta) = \frac{\Gamma(1-b)}{\Gamma(a-b+1)} F(a,b;\zeta) + \zeta^{1-b} \frac{\Gamma(b-1)}{\Gamma(a)} F(a-b+1, 2-b;\zeta). \tag{A13}$$

For instance, for $l = 1$, we get

$$\begin{aligned}
R^{l=1}_{\mathrm{in(MST)}}(r) &= \frac{r}{M\kappa} - \frac{1}{\kappa}\left(1 + \frac{\omega^2 r^3}{10M}\right)\eta^2 + \frac{i\omega r}{\kappa^2}[1 + 2\kappa + 2\kappa^2 - (1+\kappa)^2\gamma]\eta^3 - \frac{\omega^2 r^2}{\kappa}\left(\frac{7}{10} - \frac{\omega^2 r^3}{280M}\right)\eta^4 \\
&\quad - \frac{iM\omega}{\kappa^2}\left(1 + \frac{\omega^2 r^3}{10M}\right)[1 + 2\kappa + 2\kappa^2 - (1+\kappa)^2\gamma]\eta^5 \\
&\quad - \left\{\left[\frac{16875 + 120375\kappa^2 + 87075\kappa^4 + 23790\kappa^6 + 1616\kappa^8}{75(15+4\kappa^2)^2} + [1 + 2\kappa + 2\kappa^2 - (1+\kappa)^2\gamma]^2 \right.\right. \\
&\quad \left.\left. - \frac{1}{6}(1 + 6\kappa^2 + \kappa^4)\pi^2 - \frac{4}{15}\kappa^2(15 + 4\kappa^2)\ln\left(\frac{2M\kappa\eta^2}{r}\right)\right]\frac{M\omega^2 r}{2\kappa^3} - \frac{\omega^4 r^4}{\kappa}\left(\frac{151}{2520} - \frac{\omega^2 r^3}{15120M}\right)\right\}\eta^6 \\
&\quad + O(\eta^7), \\
R^{l=1}_{\mathrm{up(MST)}}(r) &= -\frac{i}{2\omega^2 r^2} - \frac{i}{4}\left(1 + \frac{4M}{\omega^2 r^3}\right)\eta^2 + \frac{M}{\omega r^2}\left(1 + \frac{\omega^2 r^3}{6M} - \gamma + i\pi\right)\eta^3 - i\left(\frac{M}{r} - \frac{\omega^2 r^2}{16} + \frac{3(5+\kappa^2)M^2}{10\omega^2 r^4}\right)\eta^4 \\
&\quad + \left[\left(\frac{1}{3} - \frac{\gamma}{2} + \frac{i\pi}{2}\right)M\omega + (1 - \gamma + i\pi)\frac{2M^2}{\omega r^3} - \frac{\omega^3 r^3}{60}\right]\eta^5 \\
&\quad + \left\{-\frac{2iM^3}{5\omega^2 r^5}(5 + 3\kappa^2) + \frac{iM^2}{15r^2}\left[-(15 + 4\kappa^2)\ln(2\omega r\eta) + 15(\gamma - i\pi)^2 - (45 + 4\kappa^2)\gamma + 30i\pi - \frac{5}{2}\pi^2 \right.\right. \\
&\quad \left.\left. + \frac{101250 + 67800\kappa^2 + 15435\kappa^4 + 848\kappa^6}{10(15+4\kappa^2)^2}\right] + \frac{iM\omega^2 r}{3}\left(2\ln(2\omega r\eta) + \gamma - \frac{61}{24}\right) - \frac{i\omega^4 r^4}{288}\right\}\eta^6 \\
&\quad + O(\eta^7),
\end{aligned} \tag{A14}$$

having rescaled the "in" solution by the constant factor $\Gamma(c)$, with

$$\nu = 1 - \left(\frac{1}{2} + \frac{2}{15}\kappa^2\right)\epsilon^2 - \frac{496125 + 680400\kappa^2 + 135990\kappa^4 + 12688\kappa^6}{189000(15+4\kappa^2)}\epsilon^4 + O(\epsilon^6). \tag{A15}$$

APPENDIX B: ENERGY FLUXES

Using the notation of Ref. [48], the energy fluxes (5.8) and (5.9) can be written as

$$\begin{aligned}
\frac{dE^\infty}{dt} &= \left(\frac{dE^\infty}{dt}\right)_N \sum_{l=1}^{\infty}\sum_{m=-l}^{l}\eta^\infty_{lm}, \\
\frac{dE^H}{dt} &= \left(\frac{dE^\infty}{dt}\right)_N 2(1-w)(1+\sqrt{1-w})y^3 \sum_{l=1}^{\infty}\sum_{m=-l}^{l}\eta^H_{lm},
\end{aligned} \tag{B1}$$

with $\eta^{H,\infty}_{l-m} = \eta^{H,\infty}_{lm}$. For small values of the dimensionless angular velocity variable y, the expansion coefficients behave as $\eta^\infty_{lm} \sim y^{l-1}$ and $\eta^H_{lm} \sim y^{2(l-1)}$, for fixed values of m. Therefore, since we have used the MST solutions up to $l = 4$, our calculations of the flux at infinity and on the horizon are accurate up to the order $O(y^{7/2})$ and $O(y^{15/2})$ beyond the lowest order, respectively. For example, for $l = 1$, the first few terms of the expansion are given by

$$\eta_{11}^{\infty}=\frac{1}{2}+\left(-\frac{13}{5}+\frac{1}{3}w\right)y+\pi y^{3/2}+\left(\frac{1123}{350}+\frac{1}{30}w-\frac{1}{6}w^2\right)y^2+\left(-\frac{26}{5}+\frac{2}{3}w\right)\pi y^{5/2}$$
$$+\left[\frac{10958}{945}-\frac{12427}{3150}w+\frac{26}{45}w^2+\frac{14}{81}w^3+\frac{2}{3}\pi^2+\left(-\frac{38}{15}+\frac{8}{15}w\right)\gamma+\left(-\frac{38}{15}+\frac{8}{15}w\right)\ln(2)\right.$$
$$\left.+\left(-\frac{19}{15}+\frac{4}{15}w\right)\ln(y)\right]y^3+\left(\frac{1123}{175}+\frac{1}{15}w-\frac{1}{3}w^2\right)\pi y^{7/2}+O(y^4),$$
$$\eta_{11}^{H}=\frac{1}{2}+\left(1-\frac{2}{3}w\right)y+\left(\frac{11}{10}-\frac{23}{30}w+w^2\right)y^3$$
$$+\left[\frac{971}{150}+\frac{347}{450}w+\frac{44}{45}w^2-\frac{130}{81}w^3+\frac{1}{2(1-w)}+\left(-\frac{19}{15}+\frac{4}{15}w\right)\ln(1-w)+\frac{1}{(1-w)^{1/2}}\left(\frac{2}{3}-\frac{1}{3}w\right)\pi^2\right.$$
$$\left.-\frac{4}{3}\gamma+\left(-\frac{58}{15}+\frac{8}{15}w\right)\ln(2)+\left(-\frac{16}{5}+\frac{8}{15}w\right)\ln(y)\right]y^4+O(y^5). \quad \text{(B2)}$$

[1] L. Barack, Gravitational self force in extreme mass-ratio inspirals, Classical Quantum Gravity **26**, 213001 (2009).
[2] Y. Mino, M. Sasaki, and T. Tanaka, Gravitational radiation reaction to a particle motion, Phys. Rev. D **55**, 3457 (1997).
[3] T. C. Quinn and R. M. Wald, An Axiomatic approach to electromagnetic and gravitational radiation reaction of particles in curved space-time, Phys. Rev. D **56**, 3381 (1997).
[4] L. Barack and A. Ori, Mode sum regularization approach for the selfforce in black hole space-time, Phys. Rev. D **61**, 061502 (2000).
[5] T. C. Quinn, Axiomatic approach to radiation reaction of scalar point particles in curved space-time, Phys. Rev. D **62**, 064029 (2000).
[6] L. Barack, Y. Mino, H. Nakano, A. Ori, and M. Sasaki, Calculating the gravitational selfforce in Schwarzschild space-time, Phys. Rev. Lett. **88**, 091101 (2002).
[7] L. Barack and A. Ori, Gravitational selfforce and gauge transformations, Phys. Rev. D **64**, 124003 (2001).
[8] S. L. Detweiler and B. F. Whiting, Self-force via a Green's function decomposition, Phys. Rev. D **67**, 024025 (2003).
[9] E. Poisson, The motion of point particles in curved spacetime, Living Rev. Relativ. **7**, 6 (2004).
[10] L. M. Burko, Self-force on static charges in Schwarzschild space-time, Classical Quantum Gravity **17**, 227 (2000).
[11] L. Barack, Self-force on a scalar particle in spherically symmetric space-time via mode sum regularization: Radial trajectories, Phys. Rev. D **62**, 084027 (2000).
[12] L. M. Burko, Self-Force on Particle in Orbit Around A Black Hole, Phys. Rev. Lett. **84**, 4529 (2000).
[13] A. G. Wiseman, The self-force on a static scalar test charge outside a Schwarzschild black hole, Phys. Rev. D **61**, 084014 (2000).
[14] H. Nakano, Y. Mino, and M. Sasaki, Self-force on a scalar charge in circular orbit around a Schwarzschild black hole, Prog. Theor. Phys. **106**, 339 (2001).
[15] L. M. Burko and Y. T. Liu, Self-force on a scalar charge in the space-time of a stationary, axisymmetric black hole, Phys. Rev. D **64**, 024006 (2001).
[16] L. Barack and A. Ori, Regularization parameters for the self-force in Schwarzschild space-time. 1. Scalar case, Phys. Rev. D **66**, 084022 (2002).
[17] S. L. Detweiler, E. Messaritaki, and B. F. Whiting, Self-force of a scalar field for circular orbits about a Schwarzschild black hole, Phys. Rev. D **67**, 104016 (2003).
[18] H. Nakano, N. Sago, and M. Sasaki, Gauge problem in the gravitational self-force. 2. First post-Newtonian force under Regge-Wheeler gauge, Phys. Rev. D **68**, 124003 (2003).
[19] W. Hikida, S. Jhingan, H. Nakano, N. Sago, M. Sasaki, and T. Tanaka, A new analytical method for self-force regularization. 1. Scalar charged particle in Schwarzschild space-time, Prog. Theor. Phys. **111**, 821 (2004).
[20] L. M. Diaz-Rivera, E. Messaritaki, B. F. Whiting, and S. L. Detweiler, Scalar field self-force effects on orbits about a Schwarzschild black hole, Phys. Rev. D **70**, 124018 (2004).
[21] W. Hikida, H. Nakano, and M. Sasaki, Self-force regularization in the Schwarzschild spacetime, Classical Quantum Gravity **22**, S753 (2005).
[22] A. C. Ottewill and B. Wardell, Quasilocal contribution to the scalar self-force: Geodesic motion, Phys. Rev. D **77**, 104002 (2008).
[23] R. Haas, Scalar self-force on eccentric geodesics in Schwarzschild spacetime: A Time-domain computation, Phys. Rev. D **75**, 124011 (2007).
[24] T. Damour, Gravitational self-force in a Schwarzschild background and the effective one body formalism, Phys. Rev. D **81**, 024017 (2010).
[25] L. Barack and N. Sago, Gravitational self-force on a particle in eccentric orbit around a Schwarzschild black hole, Phys. Rev. D **81**, 084021 (2010).

[26] N. Warburton and L. Barack, Self force on a scalar charge in Kerr spacetime: Circular equatorial orbits, Phys. Rev. D **81**, 084039 (2010).
[27] N. Warburton and L. Barack, Self force on a scalar charge in Kerr spacetime: eccentric equatorial orbits, Phys. Rev. D **83**, 124038 (2011).
[28] B. Wardell, I. Vega, J. Thornburg, and P. Diener, A Generic effective source for scalar self-force calculations, Phys. Rev. D **85**, 104044 (2012).
[29] A. C. Ottewill and P. Taylor, Static Kerr Green's function in closed form and an analytic derivation of the self-force for a static scalar charge in Kerr space-time, Phys. Rev. D **86**, 024036 (2012).
[30] I. Vega, B. Wardell, P. Diener, S. Cupp, and R. Haas, Scalar self-force for eccentric orbits around a Schwarzschild black hole, Phys. Rev. D **88**, 084021 (2013).
[31] S. Isoyama, L. Barack, S. R. Dolan, A. Le Tiec, H. Nakano, A. G. Shah, T. Tanaka, and N. Warburton, Gravitational Self-Force Correction to the Innermost Stable Circular Equatorial Orbit of a Kerr Black Hole, Phys. Rev. Lett. **113**, 161101 (2014).
[32] N. Warburton, Self force on a scalar charge in Kerr spacetime: inclined circular orbits, Phys. Rev. D **91**, 024045 (2015).
[33] M. van de Meent, Gravitational self-force on eccentric equatorial orbits around a Kerr black hole, Phys. Rev. D **94**, 044034 (2016).
[34] F. J. Zerilli, Perturbation analysis for gravitational and electromagnetic radiation in a Reissner-Nordström geometry, Phys. Rev. D **9**, 860 (1974).
[35] M. Johnston, R. Ruffini, and F. Zerilli, Gravitationally Induced Electromagnetic Radiation, Phys. Rev. Lett. **31**, 1317 (1973).
[36] M. Johnston, R. Ruffini, and F. Zerilli, Electromagnetically induced gravitational radiation, Phys. Lett. **49B**, 185 (1974).
[37] D. Bini, A. Geralico, and R. Ruffini, On the equilibrium of a charged massive particle in the field of a Reissner-Nordstrom black hole, Phys. Lett. A **360**, 515 (2007).
[38] D. Bini, A. Geralico, and R. Ruffini, Charged massive particle at rest in the field of a Reissner-Nordstrom black hole, Phys. Rev. D **75**, 044012 (2007).
[39] D. Bini, A. Geralico, and R. Ruffini, Charged massive particle at rest in the field of a Reissner-Nordstrom black hole. II. Analysis of the field lines and the electric Meissner effect, Phys. Rev. D **77**, 064020 (2008).
[40] S. Mano, H. Suzuki, and E. Takasugi, Analytic solutions of the Regge-Wheeler equation and the postMinkowskian expansion, Prog. Theor. Phys. **96**, 549 (1996).
[41] S. Mano, H. Suzuki, and E. Takasugi, Analytic solutions of the Teukolsky equation and their low frequency expansions, Prog. Theor. Phys. **95**, 1079 (1996).
[42] D. Bini and T. Damour (unpublished).
[43] T. Damour, B. R. Iyer, and A. Nagar, Improved resummation of post-Newtonian multipolar waveforms from circularized compact binaries, Phys. Rev. D **79**, 064004 (2009).
[44] S. Akcay, L. Barack, T. Damour, and N. Sago, Gravitational self-force and the effective-one-body formalism between the innermost stable circular orbit and the light ring, Phys. Rev. D **86**, 104041 (2012).
[45] S. A. Teukolsky, Perturbations of a rotating black hole. 1. Fundamental equations for gravitational electromagnetic and neutrino field perturbations, Astrophys. J. **185**, 635 (1973).
[46] W. H. Press and S. A. Teukolsky, Perturbations of a rotating black hole. II. Dynamical stability of the Kerr metric, Astrophys. J. **185**, 649 (1973).
[47] S. A. Teukolsky and W. H. Press, Perturbations of a rotating black hole. III—Interaction of the hole with gravitational and electromagnetic radiation, Astrophys. J. **193**, 443 (1974).
[48] M. Sasaki and H. Tagoshi, Analytic black hole perturbation approach to gravitational radiation, Living Rev. Relativ. **6**, 6 (2003).